Riddles, P., Blakeley, R., & Zerner, B. (1983) *Methods Enzymol. 91*, 49-60.
Russel, M., & Model, P. (1985) *Proc. Natl. Acad. Sci. U.S.A. 82*, 29-33.
Russel, M., & Model, P. (1986) *J. Biol. Chem. 261*, 14997-15005.
Shalongo, W., Ledger, R., Jagannadham, M., & Stellwagen, E. (1987) *Biochemistry 26*, 3135-3141.
Spratt, B., Hedge, P., te Hessen, S., Edelman, A., & Broome-Smith, K. (1986) *Gene 41*, 337-342.
Sung, Y.-C., Anderson, P., & Fuchs, J. A. (1987) *J. Bacteriol. 169*, 5224-5230.
Tanford, C. (1970) *Adv. Protein Chem. 24*, 1-93.
Tsang, M., & Schiff, J. (1976) *J. Bacteriol. 125*, 1923-1933.
Wilson, J., Kelley, R., Shalongo, W., Lowery, D., & Stellwagen, E. (1986) *Biochemistry 25*, 7560-7566.

Structural Domains and Conformational Changes in Nuclear Chromatin: A Quantitative Thermodynamic Approach by Differential Scanning Calorimetry†

Cecilia Balbi,‡ Maria L. Abelmoschi,‡ Luca Gogioso,‡ Silvio Parodi,‡ Paola Barboro,§ Barbara Cavazza,§ and Eligio Patrone*,§

Centro di Studi Chimico-Fisici di Macromolecole Sintetiche e Naturali, CNR, and Istituto Nazionale per la Ricerca sul Cancro, Genova, Italy

Received July 12, 1988; Revised Manuscript Received November 29, 1988

ABSTRACT: A good deal of information on the thermodynamic properties of chromatin was derived in the last few years from optical melting experiments. The structural domains of the polynucleosomal chain, the linker, and the core particle denature as independent units. The differential scanning calorimetry profile of isolated chromatin is made up of three endotherms, at ~74, 90, and 107 °C, having an almost Gaussian shape. Previous work on this matter, however, was mainly concerned with the dependence of the transition enthalpy on external parameters, such as the ionic strength, or with the melting of nuclei from different sources. In this paper we report the structural assignment of the transitions of rat liver nuclei, observed at 58, 66, 75, 92, and 107 °C. They are representative of the quiescent state of the cell. The strategy adopted in this work builds on the method developed for the investigation of complex biological macromolecules. The heat absorption profile of the nucleus was related to the denaturation of isolated nuclear components; electron microscopy and electrophoretic techniques were used for their morphological and molecular characterization. The digestion of chromatin by endogenous nuclease mimics perfectly the decondensation of the higher order structure and represented the source of several misinterpretations. This point was carefully examined in order to define unambiguously the thermal profile of native nuclei. The low-temperature transitions, centered around 58 and 66 °C, arise from the melting of scaffolding structures and of the proteins associated with heterogeneous nuclear RNA. The conformational change of the linker domain occurs at 75 °C. Finally, the endotherms at 92 and 107 °C reflect the denaturation of the core particle placed within an expanded loop and the 30-nm fiber, respectively. The stability of chromatin higher order structure appears to be enthalpy dependent, because a large decrease in the denaturation heat is associated with unfolding. Starting from these assignments, we gained an insight into the structural changes underlying the progress of the cell along the cycle. The 107 °C endotherm is dominant in both G_0 and S phase, but actively dividing hepatocytes are characterized by a reproducible broadening of the thermal profile at 100 °C, related to the regional unwinding of the 30-nm fiber occurring during transcription and DNA replication.

A few years ago (Nicolini et al., 1983) we embarked upon an investigation on the denaturation enthalpy of both calf thymus chromatin and rat liver nuclei. Our experiments revealed several intriguing features of the melting behavior of these materials. In spite of an extremely heterogeneous composition, the denaturation process resulted in strikingly simple DSC[1] profiles. Three major endotherms, having an almost Gaussian shape, were observed at 74, 90, and 107 °C for both chromatin and nuclei. In the latter case, an additional broad peak at ~58 °C was present. Moreover for isolated chromatin, the heat absorbed at 90 and 107 °C was found to increase strongly with the concentration of monovalent salt between 10 and 50 mM, where the transition from the 10-nm fiber to the helical structure occurs (Thoma et al., 1979). We drew the conclusion that DSC methods could be successfully applied in order to investigate the condensation process of

† This work was supported by the Italian National Research Council, Special Project "Oncology" (Grants 212336.44.8706642, 104348.44.8706643, and 87.01566.44), and the EEC (Grant EV4V-0036-I(A)). P.B. thanks the Italian Association for Cancer Research for a fellowship.

* Correspondence should be addressed to this author at the Centro di Studi Chimico-Fisici di Macromolecole Sintetiche e Naturali, Corso Europa 30, 16132 Genova, Italy.
‡ Istituto Nazionale per la Ricerca sul Cancro.
§ CNR.

[1] Abbreviations: DSC, differential scanning calorimetry; DNase, deoxyribonuclease; EDTA, ethylenediaminetetraacetic acid; PMSF, phenylmethanesulfonyl fluoride; BN, nuclei prepared in batch; FN, nuclei isolated in flow; NM, nuclear matrix; Tris, tris(hydroxymethyl)aminomethane; hnRNA, heterogeneous nuclear RNA; SDS, sodium dodecyl sulfate; IF, intermediate filaments; kbp, kilobase pair(s); kDa, kilodalton(s); RNase, ribonuclease.

0006-2960/89/0428-3220$01.50/0

nuclear chromatin along the cell cycle. More recently, it has been shown that the high-temperature endotherms undergo sharp changes upon mild micrococcal nuclease or DNase I digestion (Trefiletti et al., 1984; Touchette & Cole, 1985), a finding suggestive of some dependence of the denaturation enthalpy on the loss of the higher order organization of chromatin. On the whole, the above results did not permit attachment of a precise structural meaning to the transitions.

To date, the potential of DSC has not been fully exploited in cell biology as a consequence of both the insufficient reproducibility of the data and the difficulties inherent in their interpretation. Obviously, a significant advance cannot take place until the domain (or domains) which melt(s) in each endotherm has (have) been identified. Our aim here is to settle this matter in a straightforward way, by providing the bare thermal profiles with independent chemical and structural information. The chromatin fiber is subdivided into two structural supramolecular domains, the core particle and the "linker" DNA. Thus, the first point which has to be considered is the recognition of their contributions within the excess heat capacity profile; each of them, in principle, can give rise to one or more transitions because nuclear chromatin is in different conformational states. It will be shown that the endotherms at 90 and 107 °C correspond to the denaturation of the core particle placed within an unordered loop and the higher order structure, respectively. Hence, the problem of chromatin condensation can be addressed quantitatively by microcalorimetry.

Experimental Procedures

Preparation of Hepatocytes and Nuclei from Rat Liver. All the experiments were carried out at 4 °C. Male albino Sprague-Dawley rats (CD Charles River) 2–3 months old were used. Partial hepatectomy was carried out according to Grisham (1962). After in situ perfusion (Parodi et al., 1983), the liver was excised and minced in 20 mL of dissociation medium (75 mM NaCl, 24 mM Na_2EDTA, 5 mM $Na_2S_2O_5$, 1 mM PMSF, pH 7.8). The tissue was gently homogenized in a loose-fitting potter and sieved through a stainless steel grid. Hepatocytes were harvested by centrifugation at 150*g* for 4 min. The pellet was incubated for 4 min in 9 volumes of isolation buffer [dissociation medium containing 0.5% (v/v) Triton X-100]. The suspension was centrifuged at 150*g* for 3 min. This step repeated twice without incubation was followed by washing in dissociation medium. This material will be referred to as nuclei prepared in batch (BN).

Nuclei can be effectively freed of cytoplasmic debris by a continuous (in flow) extraction procedure (Barboro et al., 1987). A dilute (0.5×10^6 cells/mL) suspension of hepatocytes is pumped into a small-volume (0.05 cm^3) T-shaped mixing chamber together with an equal volume of dissociation medium containing 1% (v/v) Triton X-100 and conveyed through a Teflon tube 0.1 cm in diameter. Its length l and the volume rate of flow Q are the critical factors governing the efficiency of the separation process, which depends on both the incubation time and the application of shear forces. Optimum operating conditions are $l = 2 \times 10^2$ cm and $Q = 1$ cm^3/min. Nuclei isolated in flow (FN) were collected by centrifugation at 5000*g* for 30 min.

A crude nuclear fraction was obtained at low ionic strength by resuspending pelleted hepatocytes in 10 volumes of 0.2 mM Na_2EDTA (final Na^+ concentration 10 mM). Lysis was carried out under gentle shaking for different lengths of time (0–3 h). Centrifugation at 150*g* for 5 min yielded a nuclear pellet and a supernatant, which in some experiments was further fractionated at 10000*g* for 15 min.

Preparation of the Nuclear Matrix. The nuclear matrix (NM) was obtained from BN according to the double-detergent procedure (Capco et al., 1982). Alternatively, nuclei were resuspended in 9 volumes of 10 mM NaCl, 3 mM $MgCl_2$, and 10 mM Tris (pH 7.4), and DNase I (Sigma) was added to a final concentration of 0.4 mg/mL. The digestion was carried out at 25 °C for 60 min and stopped by addition of Na_2EDTA and chilling on ice. This preparation retains most of the hnRNA-associated proteins.

Micrococcal Nuclease Digestion. BN were resuspended in 75 mM NaCl, 1 mM $CaCl_2$, and 2.5 mM Tris (pH 8). The digestion was carried out as described by Noll et al. (1975) at a DNA concentration of 1.2 mg/mL in the presence of either 5 or 15 units/mL micrococcal nuclease (Sigma) and stopped after 20 or 180 s, respectively. For the purpose of determining the DNA chain-length distribution, the samples were centrifuged at 5000*g* for 10 min, and the pellet was extracted with 20 volumes of digestion buffer containing 2 mM Na_2EDTA, and centrifuged as above. The supernatants were combined and processed as described below.

Gel Electrophoresis of DNA Fragments and Nuclear Proteins. Nuclear pellets, as well as fractions from nuclease-digested or endogenous nuclease degraded samples, were deproteinized at 37 °C for 2 h with 0.25 mg/mL proteinase K (Serva) in 5 mM Na_2EDTA containing 0.5% (w/v) SDS. After ethanol precipitation, the samples were run for 2 h at 5 V/cm on 0.6% agarose gel slabs in 90 mM Tris–borate buffer (pH 8) containing 2 mM Na_2EDTA. The slabs were stained with 1 μg/mL ethidium bromide and photographed in an LKB 2011 transilluminator. Negative images were enlarged on a 3M X-ray film and the densitometric profiles recorded at 500 nm with a Beckman DU-8 spectrophotometer. Gel electrophoresis of the NM proteins was carried out on 12.5% SDS–polyacrylamide gels (Laemmli, 1970).

Chemical Assay of DNA, RNA, and Proteins. The assay of DNA concentration was performed according to the fluorometric procedure of Fiszer-Szafarz et al. (1981). RNA and nuclear proteins were determined by the orcinol (Ceriotti, 1955) and Coomassie brilliant blue G-250 (Bio-Rad Protein Assay) methods, respectively.

Electron Microscopy. Nuclei and chromatin fragments obtained by hypotonic swelling were adsorbed on a phospholipid monolayer as already described (Cavazza et al., 1983) and shadowed with platinum at an angle of 16° from two directions 90° apart. For routine observations on the morphology of nuclei, a droplet of the suspension was applied to a carbon-coated grid, the excess solution removed by filter paper, and the sample stained with 1% uranyl acetate. Owing to the presence of the nonionic detergent, which greatly enhances the wettability of the carbon surface, the spread nuclei were free from gross distortions. A Siemens 102 electron microscope operating at 80 kV was used.

Calorimetry. DSC experiments were performed as already described (Nicolini et al., 1983) with a Perkin-Elmer DSC 7 microcalorimeter. Prior to the determination, the material was resuspended in dissociation medium and pelleted by centrifugation at 10000*g* for 5 min. The scan rate was 5 °C/min. The samples used in the experiments contained from 0.3 to 0.5 mg of DNA.

Deconvolution of the excess heat capacity curves into Gaussian transitions has been carried out as follows. Starting from the function

$$y(T) = \sum_{k=1}^{5} A_k \exp\left[-\frac{(T - \bar{T}_k)^2}{\sigma_k^2}\right] \quad (1)$$

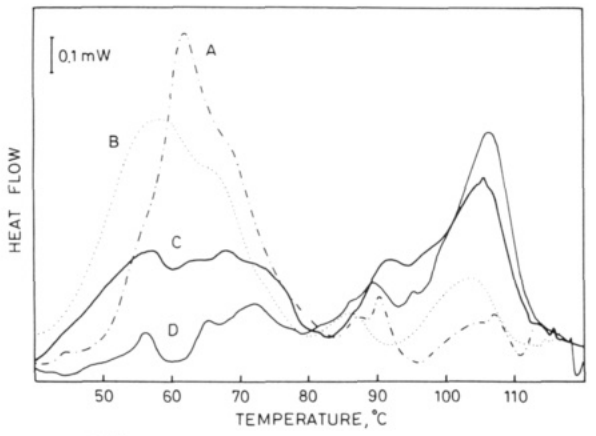

FIGURE 1: Differential scanning calorimetry profiles of hepatocytes (A), the nuclear fraction obtained from hepatocytes by hypotonic shock (B), nuclei prepared in batch (C), and nuclei isolated in flow (D).

the best evaluation of the parameters A_k, $\bar{T}_k$, and σ_k has been obtained in the least-squares sense; in other words, we calculate the set of parameters which minimizes the error function

$$\sum_{i=1}^{N} \frac{(y_{it} - y_{im})^2}{y_{it}} \qquad (2)$$

where y_{im} are the experimental values of the excess heat capacity at T_i ($i = 1, ..., N$) and y_{it} are the corresponding theoretical values.

The algorithm used (Barabino & Marchesi, 1978) is a very simple iterative procedure; i.e., representing our function in a N-dimensional space ($N = 15$), at each step the method, by traveling a certain distance along each axis, carries out two tentatives to minimize the error function. This algorithm was applied with a program written in FORTRAN for a Hewlett-Packard 1000 computer.

Results

Denaturation Profile of Nuclei in Relation to the Isolation Procedure. Figure 1 reports a comparison among the DSC profiles of hepatocytes (A), nuclei obtained by hypotonic shock (B), and BN and FN (C and D, respectively). This sequence shows the gradual decrease in the heat absorbed between 40 and 80 °C and the increase in the endotherms at ~90 and 107 °C as the amount of cytoplasmic material reduces.

The micrograph in Figure 2A shows a nucleus isolated immediately after resuspension of the hepatocytes in 0.2 mM Na_2EDTA. A network of chromatin fibers, connected with laminar fragments 10–20 nm thick (inset), surrounds a residual compact core. Thus, for hypotonic nuclei the envelope in association with cytoplasmic debris largely contributes to the thermal effect centered around 60 °C. When the nuclear membrane is removed in the presence of Triton X-100, a small fraction (~0.2) only of the total denaturation heat is invested in the low-temperature region, but some quantitative difference between scans C and D is still observed. BN have a higher thermal response, with a broad peak at 57 °C and a less distinct transition between 60 and 70 °C; FN show sharper endotherms at 56.4 and 66.2 °C. As regards the melting behavior beyond 70 °C, either isolation procedure leads substantially to the same profile, with main absorption peaks at ~90 and 107 °C except for the transition at 73 °C, which for BN is less resolved owing to its overlapping with the diffuse effect occurring at lower temperatures. The more pronounced heat absorption observed for BN is related to a higher protein content. The DNA:RNA:protein weight ratio is 1:0.1:4.0 for BN, to be compared with 1:0.1:2.5 determined for FN. The micrograph shown in Figure 2B offers an insight into this matter. A thin halo of fibers spreads from the surface of FN. BN are embedded in a denser matrix, which cannot be adequately focused in the electron microscope. This observation together with gel electrophoretic analysis of the nuclear proteins (not shown) indicates that variable amounts of tenaciously bound intermediate filaments (IF) are isolated with nuclei, so causing the minor discrepancies pointed out above.

The DSC experiments reported in this paper have been carried out on BN. Their accuracy is sufficient to warrant a quantitative treatment of the data. Nevertheless, it is instructive to comment briefly on the extremely reproducible results which can be obtained with the cleaner FN. A few thermograms are collected in Figure 3; the transitions are marked by Roman numerals. In four experiments out of five they occur at 56.4 ± 0.3, 66.3 ± 0.2, 72.7 ± 0.8, 89.7 ± 0.4, and 106.6 ± 0.2 °C (mean ± standard deviation). The profiles match well and, after normalization with respect to the content of DNA, can be averaged with an uncertainty of ±5%. In the arrowed scan the high-temperature endotherm occurs at 104.5 °C. This value corresponds to the onset of chromatin digestion by endogenous nuclease, a crucial point that will be considered in the next section.

Ionic Strength of the Isolation Buffer Controls the Rate of Decay of the 107 °C Endotherm. BN or nuclei prepared by hypotonic shock were incubated for different times in the isolation buffer and the thermal profiles recorded. The results are shown in Figure 4. After resuspension in dissociation

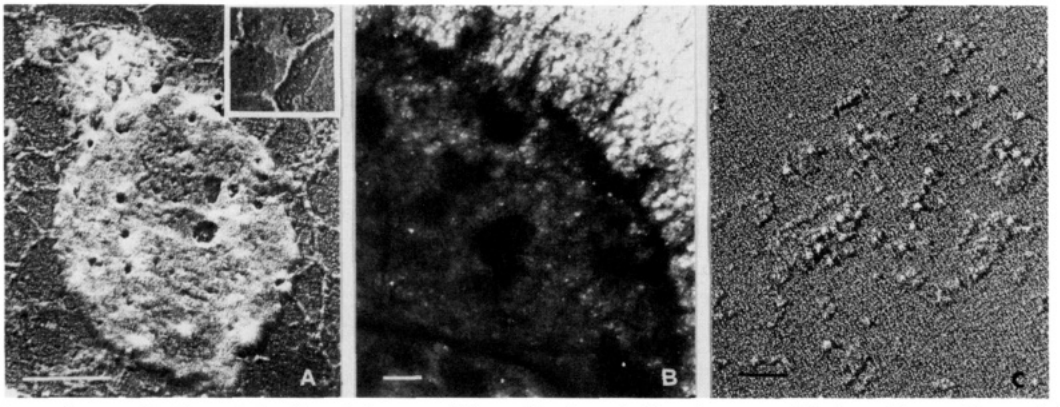

FIGURE 2: Electron microscopic characterization of the materials used in the calorimetric scans. (A) A swollen nucleus and (C) unordered polynucleosomal chains observed immediately after resuspension of the hepatocytes in 0.2 mM Na_2EDTA. The inset in (A) shows 10 nm thick laminar fragments. The samples were adsorbed on a phospholipid monolayer and shadowed with platinum. Inverted prints. (B) The edge of a nucleus isolated in flow, showing a halo of intermediate filaments. Negative staining with uranyl acetate. The bar is 1 μm in (A) and (B) and 0.1 μm in (C).

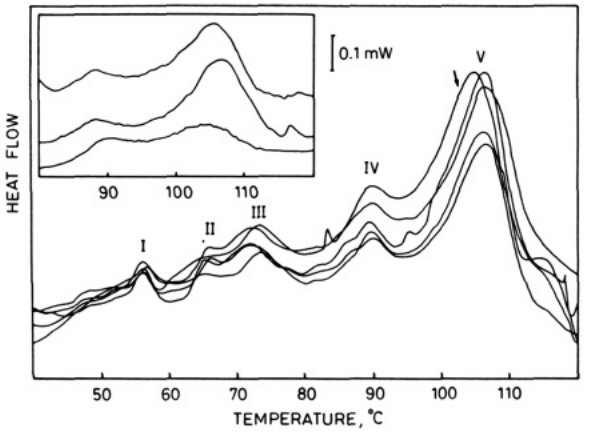

FIGURE 3: Comparison among the thermal profiles of different preparations in flow of nuclei. The inset shows the high-temperature region of the thermogram of nuclei obtained 20 h after partial hepatectomy according to the same procedure.

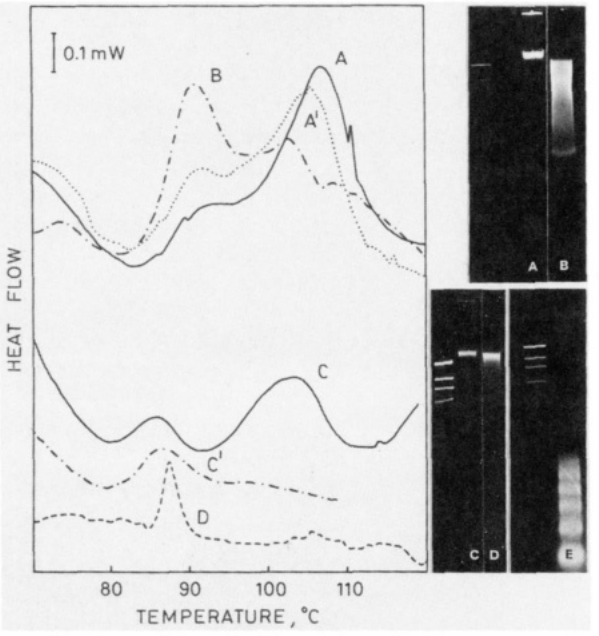

FIGURE 4: Decay of the 107 °C endotherm in the presence of 0.13 M (scans A, A′, and B) and 10 mM (scans C, C′, and D) Na^+. The corresponding agarose gel electrophoretic patterns of the DNA are indicated by the same capital letter. Markers are *Hin*dIII digests of λDNA.

medium (Na^+ concentration 0.13 M) and a 3-h incubation, we observe a slight decrease in the peak temperature T_m of endotherm V (scans A and A′), while the electrophoretic profile of DNA on agarose gels does not show any change with respect to the experiment at $t = 0$ (lane A); the band occurring beyond 40 kbp is an artifact arising from mechanical disrupture. After 72 h, we observe both a large passage of transition heat from V to IV and a further decrease in T_m^V, while the electrophoretic profile indicates a continuous and extensive breakdown of the duplex; its most probable chain length reduces to 9.4 kbp. For nuclei obtained by hypotonic shock in 0.2 mM Na_2EDTA (final Na^+ concentration 10 mM), the decay of the 107 °C endotherm becomes very fast; at $t = 0$ the pellet from the centrifugation at 150*g* (see Experimental Procedures and Figure 2A) melts in two broad transitions (scan C) as already described. Endogenous nuclease activity, however, rises immediately after swelling. The electron micrograph reported in Figure 2C shows that the corresponding supernatant consists of unordered polynucleosomal chains as well as of oligonucleosomes. These

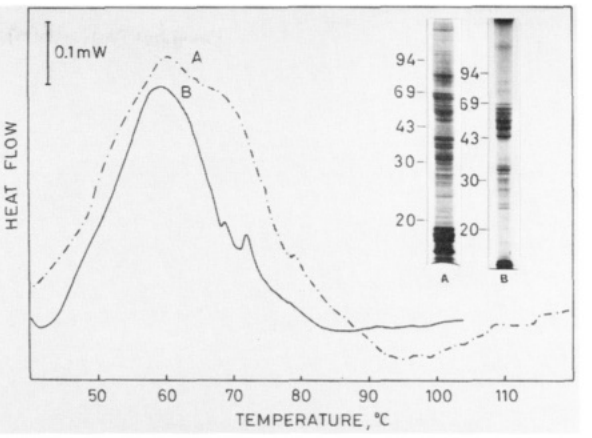

FIGURE 5: Denaturation of the residual nuclear structures isolated by Triton X-100 wash and DNase I digestion (A) and by the double-detergent method (B). The one-dimensional electrophoretic analysis of the protein composition on 12.5% SDS–polyacrylamide gels is shown (lanes A and B). The molecular weight of standard proteins expressed in kDa is reported on the left.

components can be recovered by centrifugation at 10000*g* for 15 min in two fractions, namely, a smeared band (lane D) and an oligonucleosomal ladder centered around three nucleosomes (lane E). The heat absorption curve of the former (scan D) shows nothing but an endotherm at 87 °C, with possible residual effects at 75 and 105 °C. After a 3-h incubation no appreciable heat absorption can be detected beyond 90 °C for the pellet from the centrifugation at 150*g* (scan C′). The quantitative analysis of scans C′ and D is subjected to quite a high degree of error, because the samples used in the experiments contained an amount of DNA as low as 0.03 mg. Qualitatively, however, they confirm that endogenous nuclease digestion causes an apparent heat "pumping" from V to IV and show that when the effect becomes severe, so that cuts are introduced within neighboring nucleosomes, heat absorption occurs almost around 85 °C.

In a recent paper Walker et al. (1986) approached the problem of the structure of nuclear chromatin by using digestion experiments at different ionic strengths as the probe. They observed that the high level of endogenous nuclease of rat liver nuclei complicates the interpretation of the results; when nuclei are isolated in the presence of a low concentration of monovalent cation, almost the whole DNA is released. The explanation is that a progressive unfolding of the higher order structure occurs with decreasing ionic strength; the conformational change enhances, in turn, the effect of endogenous nuclease, because the number of sites available for digestion increases.

Our calorimetric data fully confirm this sequence of physical and chemical events. Touchette et al. (1986) were led by their experiments to favor the view that the endotherm at ~88 °C predominates the calorimetric profile of nuclei from nondividing cells. On the contrary, the opposite situation is invariably observed, provided that the activity of endogenous nuclease is suppressed. As a rule, the absence of any transition around 107 °C has to be regarded with suspicion, and no statement on the organization of chromatin should be drawn in the absence of a careful check on the integrity of DNA.

NM and hnRNA-Associated Proteins Melt in Transitions I and II. The finding that no heat absorption peak occurs below 70 °C for isolated chromatin (Nicolini et al., 1983) serves as an indication that I and II result from the denaturation of scaffolding structures. The melting of these latter is shown in Figure 5. When nuclei are digested with DNase I only, we observe an inflection point at 57 °C, a peak at 60.5

Table I: Thermodynamic Parameters of the Transitions Observed for Native and Micrococcal Nuclease Digested Nuclei

	ΔH_m^I [kcal·(mol·bp)$^{-1}$]	T_m^I (°C)	ΔH_m^{II} [kcal·(mol·bp)$^{-1}$]	T_m^{II} (°C)	ΔH_m^{III} [kcal·(mol·bp)$^{-1}$]	T_m^{III} (°C)	ΔH_m^{IV} [kcal·(mol·bp)$^{-1}$]	T_m^{IV} (°C)	ΔH_m^V [kcal·(mol·bp)$^{-1}$]	T_m^V (°C)
control nuclei[a]	3.1 ± 0.5	58.0 ± 1.2	0.5 ± 0.2	65.6 ± 0.6	3.8 ± 0.4	75.1 ± 1.5	3.8 ± 0.3	92.1 ± 1.0	7.8 ± 0.4	107.0 ± 0.4
digested nuclei										
5 units/mL for 20 s	1.2	54.1	0.7	60.9	3.2	68.2	4.4	90.3	1.5	102.6
15 units/mL for 180 s	1.1	54.0	1.0	60.9	2.5	68.0	5.8	85.0	0.2	93.4

[a] The values are the mean of five determinations ± standard deviation.

°C, and a pronounced shoulder at 66 °C (scan A). One-dimensional analysis of the protein composition on SDS–polyacrylamide gels (lane A) shows two major subsets of bands in the ranges 69–45 and 40–30 kDa. This pattern indicates that almost all the hnRNA-associated proteins are present in addition to lamins. When the NM is prepared according to a classical protocol (Capco et al., 1982) including both RNase digestion and a high-salt wash, a drastic depletion of proteins in the region centered around 35 kDa occurs (lane B). This material denatures (scan B) in an endotherm at 58–60 °C, with a tail at ~66 °C. At this temperature we observe a large enthalpy loss. We conclude that the denaturation of the hnRNA-associated proteins occurs mainly around 66 °C, where the largest thermal response to RNase digestion is observed. Furthermore, these results suggest that lamins melt at ~58 °C close to IF. This tentative assignment largely rests on the comparison with the melting behavior of both BN and FN (Figure 1), for which the value of the enthalpy around 60 °C appears to be correlated with the amount of IF.

Micrococcal or Endogenous Nuclease Digestion Results in a Large Decrease in the Overall Transition Enthalpy of Chromatin. BN were digested with micrococcal nuclease (5 or 15 units/mL for 20 or 180 s, respectively). The excess heat capacity curves are reported in Figure 6. The values of both ΔH_m and T_m for the different transitions are listed in Table I.

Both V and IV exhibit an extremely large response to DNA chain scission. In going from control to mildly digested (5 enzyme units for 20 s) nuclei (Figure 6A,B), the value of ΔH_m^V passes from 7.8 to 1.5 kcal·(mol·bp)$^{-1}$. Furthermore, the degradation process brings about a depression in T_m^V equal to 5 °C. At this stage, the most probable chain length of the DNA is 4.5 kbp (lane B in Figure 6C). Upon digestion in the presence of 15 enzyme units, transition V is no longer detectable in the thermogram (Figure 6C). The presence of small amounts of material melting at high temperature can be inferred from the skewed shape of the main endotherm at 85 °C resulting in a weak component at 93 °C after deconvolution. The most probable chain length of the DNA drops to 2 kbp (lane C). The trend of transition IV as a function of the extent of DNA degradation is at variance. T_m^{IV} decreases from 92 to 85 °C, while the value of ΔH_m^{IV} apparently increases from 3.8 to 5.8 kcal·(mol·bp)$^{-1}$.

A passage of denaturation heat from 107 °C to a lower temperature has been noted early (Trefiletti et al., 1984; Touchette & Cole, 1985) suggesting that transition IV is related to the unfolding of the higher order structure. The explanation of the enthalpy increase of IV is as follows. The large chromatin stretches which are released in the initial stages of digestion have a stability comparable with the one of the native state which unfolds in IV, so that the enthalpy becomes more positive as the cleavage products accumulate; on the other hand, these fragments undergo a continuous

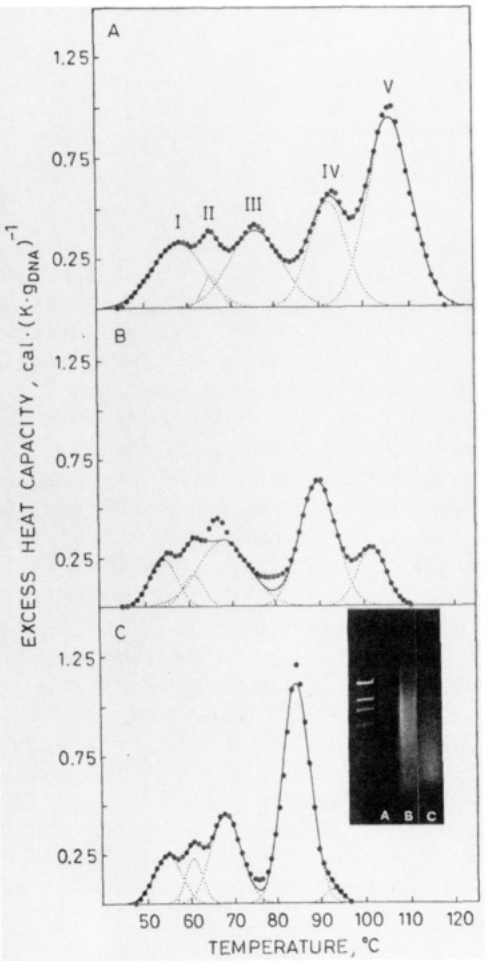

FIGURE 6: Melting profiles of nuclei digested by micrococcal nuclease: (A) control nuclei; (B) 5 units/mL for 20 s; (C) 15 units/mL for 180 s. The chain-size distribution of the DNA fragments has been obtained by densitometry of the agarose gels (lanes B and C). Molecular weight markers are as in Figure 4.

reduction of chain size, which is reflected in the progressive lowering of T_m^{IV} down to 85 °C. Because at this limiting temperature only short unordered polynucleosomal chains unfold, as already observed in the case of endogenous nuclease digestion, the transition can be conveniently taken as a reference state to describe the melting of more complex structures and will be indicated in the following by the subscript d. For convenience in the exposition, we disregard the fact that the endotherm occurring between 90 and 85 °C should be more properly termed IV + IV_d, rather than IV.

The data reported in Table I entail a puzzling question; namely, the increase in ΔH_m^{IV} [2 kcal·(mol·bp)$^{-1}$] is much less than the decrease observed for ΔH_m^V [7.6 kcal·(mol·bp)$^{-1}$], at variance with a previous suggestion (Touchette & Cole, 1985). The ease with which chromatin fragments are released

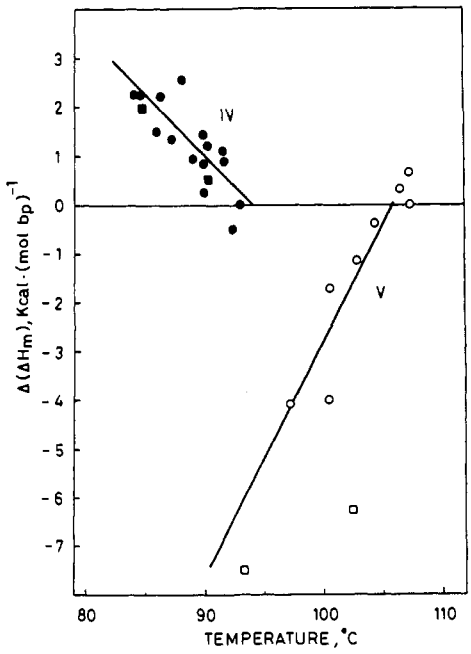

FIGURE 7: Increments of ΔH_m^{IV} (full circles) and ΔH_m^{V} (open circles) for nuclei incubated in the presence of 0.13 M Na^+ as a function of T_m^{IV} and T_m^{V}. The solid lines represent the best linear least-squares fit of the data. The results of micrococcal nuclease digestion experiments (full and open squares) are shown for comparison.

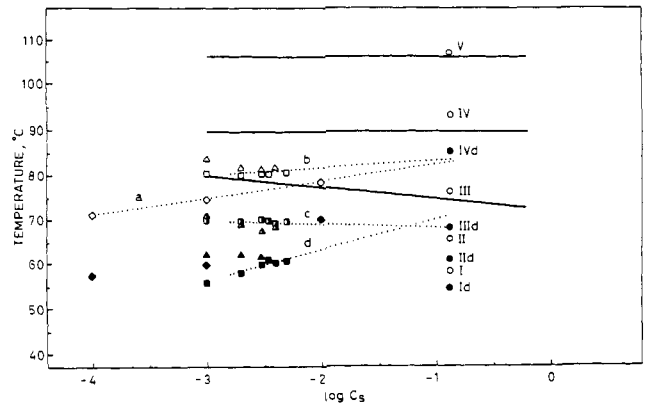

FIGURE 8: Experimental values of the melting temperatures of the transitions observed for nuclei and degraded chromatin plotted against the logarithm of the monovalent counterion concentration. Data for the isolated core particle are shown as well. Whole (△, ▲, ▲) and core chromatin (□, ■, ■) from Fulmer and Fasman (1979); core particle (◇, ◆) from Weischet et al. (1978); control and digested nuclei (○, ●) from this work. The endotherms are indicated by Roman numerals. Transitions observed for native chromatin (—) are from Nicolini et al. (1983).

from digested nuclei could result in an apparent decrease in the thermal effect. We designed additional experiments in order to circumvent this possible source of error. Aliquots of the same nuclear pellet were transferred into calorimetric capsules and the thermal profile recorded at different incubation times. In this way, the eventual leakage of chromatin during the final centrifugation step was avoided. In order to have a better appreciation of the results, the increments of the transition enthalpies with respect to the values of control nuclei, $\Delta(\Delta H_m)$, are plotted against T_m^{V} and T_m^{IV} in Figure 7. The data are consistent with those relative to micrococcal nuclease digestion, except the point corresponding to transition IV for nuclei treated with 5 enzyme units for 20 s (Figure 6B). As expected, $\Delta(\Delta H_m^{V})$ is negative and decreases sharply with decreasing T_m^{V}; $\Delta(\Delta H_m^{IV})$ is positive and increases with decreasing T_m^{IV}. The comparison of $\Delta(\Delta H_m^{V})$ between 107 and 93 °C, where transition V vanishes, with $\Delta(\Delta H_m^{IV})$ between 92 and 85 °C ($T_m^{IV_d}$) does confirm that a large [~4 kcal·(mol·bp)$^{-1}$] enthalpy loss is associated with the degradation of nuclear chromatin.

Discussion

Structural Assignment of the Thermal Transitions of Digested Nuclei. A well-established point is that scaffolding structures only denature in transitions I and II. Micrococcal nuclease digestion brings about an appreciable depression in ΔH_m^{I} and T_m^{I}. Thus, the stability of the nuclear lamina appears to depend on the integrity of chromatin and/or RNA. This result indicates that the relationship between the organization of the genome and the architecture of the nucleus, an outstanding problem in cell biology (Hyde, 1982), can be investigated by DSC.

For extensively digested nuclei III_d and IV_d lend themselves to an immediate interpretation, because the most probable size of the chromatin fragments is as low as ten nucleosomes so that the formation of the higher order structure cannot be observed. Therefore, the transitions can be attributed to the basic domains of chromatin, the linker, and the core particle, which in the unordered chain unfold as independent units. For the purpose of confirming this hypothesis, a few relevant literature results obtained on isolated chromatin will be reexamined. The paper by Weischet et al. (1978) reports early observations on the denaturation of the core particle. The transition is biphasic in the limit of zero concentration of added electrolyte, but with increasing ionic strength it becomes monophasic, and 100 bp of DNA and core histones are denatured almost simultaneously, thereby approaching the behavior which is expected for a highly cooperative process.

A number of results of various authors, obtained either by direct DSC methods or by optical melting, on the core particle as well as on digested chromatin are collected in Figure 8 and compared with the transitions reported in the present work for both native and extensively digested BN. The points in the diagram correspond to pairs of intensive variables (T_m and the monovalent counterion concentration C_s) which define the stability of a given domain. Recalling that DNA is a highly charged "rod" which dominates over the electrostatic properties of chromatin and taking into account the proportionality between its denaturation temperature and log C_s (Record, 1975), the straight lines marked by small letters in the plot will adequately represent the dependence of T_m of different chromatin domains on the concentration of added electrolyte, so affording an objective criterion to sort out the transitions. In the simplest case, the transition temperatures (Weischet et al., 1978) of the core particle subdomain melting in a cooperative fashion (open rhomboids) can be extrapolated, along line a, to a point at log C_s = −0.88 coincident, within the experimental error, with transition IV_d. The full rhomboids correspond to the low-temperature transition, which vanishes at $C_s \sim 10$ mM.

We can now take advantage of the careful experiments by Fulmer and Fasman (1979) on the optical melting of digested chromatin associated with (whole) or depleted of (core) H1 histone. The data at C_s = 1 mM have not been taken into account because a conformational change in core chromatin has been observed at this ionic strength (Fulmer & Fasman, 1979). A high-temperature peak at ~82 °C is observed for both core and whole chromatin (open squares and triangles, respectively). The core particle DNA melts in these transitions, and we expect that either set of data can be extrapolated to transition IV_d, as actually happens (line b). The attribution

of transition III_d to the linker can be confirmed likewise. Briefly, line c accounts for the behavior of both a 40 bp long stretch of core DNA and, more importantly, the linker associated with H1 (half-full squares and triangles, respectively). These data correlate very well with endotherm III_d. In addition, the stability of the extended linker region, melting in the low-temperature transition of core chromatin (full squares), increases sharply with C_s according to line d, which at log C_s = −0.88 assumes a value (70 °C) very close to $T_m^{III_d}$ (68 °C).

The transition marked by full triangles is of minor relevance for the purpose of the present discussion; Fulmer and Fasman (1979) suggested that it could arise from a domain located at the boundary between core and linker DNA, which disappears in the course of the salt-induced nucleosome assembly.

Nature of Transitions III, IV, and V: Their Relationship with Chromatin Higher Order Structure. The pseudo phase diagram discussed above provides a rationale for filling the gap among optical and calorimetric measurements. It cannot offer, however, any insight into the nature of the transitions observed for intact nuclei, which are opaque objects. The trend of nuclease digestion indicates that III_d has its native counterpart in III, while IV_d arises from the disruption of the structures melting in IV and V. If one assumes that each Gaussian endotherm is due to the unfolding of a single domain, then III has to be attributed to the linker, IV and V to the core particle, partitioned between two different chromatin conformations. Furthermore, because a large loss of denaturation heat goes with the digestion process, the stability of these latter largely depends on the enthalpy term in the Gibbs free energy.

The attribution of III to the linker rests principally on the reference to III_d. The major effect associated with digestion is a large decrease (~7 °C) in T_m^{III} which cannot arise from the chain scission per se; recently (Balbi et al., 1988), we were able to demonstrate that the equilibrium decondensation of nuclear chromatin induces an equivalent depression in the absence of DNA breaks. Therefore, the stability of the linker is related with the unfolding of the higher order structure, a conclusion which appears very plausible from the conformational standpoint.

Transitions IV and V reveal the existence of a universal organization of the polynucleosomal chain within the resting nucleus, in that they occur at the same temperature for all the cells investigated. Another important thermodynamic property is the invariance of T_m^{IV} and T_m^{V} during the conformational changes as observed for the salt-induced refolding of calf thymus chromatin (full lines in Figure 8). This is the behavior expected for linear systems which undergo a cooperative change from an unordered to a highly ordered state.

The high values of T_m^{V} and ΔH_m^{V} indicate that the bulk of chromatin in resting cells is organized in a very stable structure. No further progress, however, in the understanding of the conformational aspects could be achieved without additional criteria. The crucial step to the complete analysis of the thermogram is the recognition of the relationship between IV and V, and we carried out experiments specifically designed to examine this point (Balbi et al., 1988). The intercalative agent ethidium bromide decondenses the higher order structure (Bordas et al., 1986); nuclei were equilibrated with ethidium and the thermal profiles recorded as a function of r, the ratio of bound dye to DNA phosphate. The transition from the 30- to the 10-nm fiber, as detected by electron microscopy, occurs around r = 0.04 and goes with a sharp increase in ΔH_m^{IV} [3 kcal·(mol·bp)$^{-1}$] comparable with the decrease in ΔH_m^{V} [4.4 kcal·(mol·bp)$^{-1}$]. The picture thus emerges that V and IV are closely related and correspond to the core particle placed within a higher order (more condensed) and a looser chromatin structure, respectively. This conformational change can be immediately distinguished from spurious effects arising from chromatin degradation, because both T_m^{V} and T_m^{IV} remain unchanged in the course of the process.

Extremely difficult to interpret is the large enthalpy loss associated with the complete disorganization of the fiber. Because ΔH_m for DNA increases with increasing T_m, one could expect, on the basis of a previous estimate obtained for core particle DNA (Bina et al., 1980), that 3.7 kcal·(mol·bp)$^{-1}$ are lost in going from V to IV_d. It has been recently shown, however (Chipev & Angelova, 1983), that for long-chain DNA the slope of the plot of ΔH_m against T_m is small, so that the above correction should not exceed 1 kcal·(mol·bp)$^{-1}$. This means that the difference between $\Delta(\Delta H_m^{V})$ and $\Delta(\Delta H_m^{IV})$ reflects the enthalpy of formation of the fiber rather than the state of the denatured duplex.

Several physical factors can be invoked in order to explain the high denaturation enthalpy of condensed chromatin. The packaging of the nucleosomes in the higher order structure may involve a large molecular rearrangement of the core histones, as well as the interaction of these latter with portions of linker DNA.

Chromatin Structure in Actively Dividing Cells. Because chromatin decondensation is associated with both transcriptional activity and DNA replication, the high-temperature peaks must hold the major structural differences between cycling and resting cells. Either process involves local unfolding, which can to some extent propagate to adjacent regions. According to the assignments discussed above, we expect, for dividing cells, a broadening of the 107 °C endotherm toward lower temperatures, as a consequence of the displacement of nucleosomes from condensed and inactive chromatin domains to the open configurations which are at work. These latter represent in any phase of the cell cycle a small fraction of the genome, so that one can in addition predict the thermal profile to be only slightly affected by the functional state of the cell.

The inset in Figure 3 reports a few scans of nuclei from rat liver isolated in flow 20 h after partial hepatectomy. At this time, 30% of the hepatocytes are in S phase (Grisham, 1962). Inspection of the curves shows that they could be hardly resolved in two Gaussian components. The existence of a hidden endotherm at ~100 °C must be postulated in order to account for the actual trend. It is just this subtle difference with respect to nondividing hepatocytes which contains the significant information on the structural changes underlying the progress through the cell cycle.

A recent paper by Almagore and Cole (1987) deals with a DSC study on terminally differentiated cells. For all the systems examined, a complete loss of the transition at 105 °C, compensated by the increase in the enthalpy at 88 °C, has been found. Noting that this result is in line with their previous observations on nuclei from mature tissues (Touchette et al., 1986), these authors reasoned that the 105 °C endotherm represents the potential of the cell to divide. This potential should ultimately reside in DNA supercoiling.

The experiments reported in the present paper support the opposing view that the high-temperature endotherm bears no relationship with DNA replication. On the contrary, this transition is dominant in G_0. For instance, it is sharply defined in the thermogram of nuclei from calf thymus as well. As far as the more speculative point is concerned, DNA supercoiling is essential for viral DNA replication, but in eukaryotic cells

all the superhelical turns are restrained in nucleosomes (Sinden et al., 1980).

The striking decondensation which chromatin undergoes in terminally differentiated cells cannot at present be explained within the framework of models relating structure with function; what might be the genetic program requiring such a large rearrangement respresents a difficult question. A close analysis of this effect should, however, take into account the possible interference of an extensive digestion process.

References

Almagor, M., & Cole, R. D. (1987) *J. Biol. Chem. 262*, 15071-15075.

Balbi, C., Abelmoschi, M. L., Zunino, A., Cuniberti, C., Cavazza, B., Barboro, P., & Patrone, E. (1988) *Biochem. Pharmacol. 37*, 1815-1816.

Barabino, G., & Marchesi, M. (1978) Rapporto Interno, Vol. 5, pp 1-12, Laboratorio Circuiti Elettronici, Genova, Italy.

Barboro, P., Cavazza, B., Patrone, E., Zunino, A., Abelmoschi, M., L., & Balbi, C. (1987) *Boll.—Soc. Ital. Biol. Sper. 8*, 667-674.

Bina, M., Sturtevant, J. M., & Stein, A. (1980) *Proc. Natl. Acad. Sci. U.S.A. 77*, 4044-4047.

Bordas, J., Perez-Grau, L., Koch, M. H. J., Vega, M. C., & Nave, C. (1986) *Eur. Biophys. J. 13*, 157-173.

Capco, D. G., Wan, K. M., & Penman, S. (1982) *Cell (Cambridge, Mass.) 29*, 847-858.

Cavazza, B., Trefiletti, V., Pioli, F., Ricci, E., & Patrone, E. (1983) *J. Cell Sci. 62*, 81-102.

Ceriotti, G. (1955) *J. Biol. Chem. 214*, 59-70.

Chipev, C. C., & Angelova, M. I. (1983) *Int. J. Biol. Macromol. 5*, 252-253.

Fiszer-Szafarz, B., Szafarz, D., & Guevara de Murillo, A. (1981) *Anal. Biochem. 110*, 165-170.

Fulmer, A. W., & Fasman, G. D. (1979) *Biopolymers 18*, 2875-2891.

Grisham, J. W. (1962) *Cancer Res. 22*, 842-849.

Hyde, J. E. (1982) *Exp. Cell Res. 140*, 63-70.

Laemmli, U. K. (1970) *Nature (London) 227*, 680-685.

Nicolini, C., Trefiletti, V., Cavazza, B., Cuniberti, C., Patrone, E., Carlo, P., & Brambilla, G. (1983) *Science (Washington, D.C.) 219*, 176-178.

Noll, M., Thomas, J. O., & Kornberg, R. (1975) *Science (Washington, D.C.) 187*, 1203-1206.

Parodi, S., Pala, M., Russo, P., Balbi, C., Abelmoschi, M. L., Taningher, M., Zunino, A., Ottaggio, L., Deferrari, M., Carbone, A., & Santi, L. (1983) *Chem.-Biol. Interact. 45*, 77-94.

Record, M. T., Jr. (1975) *Biopolymers 14*, 2137-2158.

Sinden, R. R., Carlson, J. O., & Pettijohn, D. E. (1980) *Cell (Cambridge, Mass.) 21*, 773-783.

Thoma, F., Koller, Th., & Klug, A. (1979) *J. Cell Biol. 83*, 403-427.

Touchette, N. A., & Cole, R. D. (1985) *Proc. Natl. Acad. Sci. U.S.A. 82*, 2642-2646.

Touchette, N. A., Anton, E., & Cole, R. D. (1986) *J. Biol. Chem. 261*, 2185-2188.

Trefiletti, V., Balbi, C., Abelmoschi, M. L., Cavazza, B., Parodi, S., & Patrone, E. (1984) Abstracts of the 8th International Biophysics Congress, Bristol, U.K., Abstr. 22.

Walker, P. R., Sikorska, M., & Whitfield, J. F. (1986) *J. Biol. Chem. 261*, 7044-7061.

Weischet, W. O., Tatchell, K., Van Holde, K. E., & Klump, H. (1978) *Nucleic Acids Res. 5*, 139-160.

Interactions of the Dimethyldiazaperopyrenium Dication with Nucleic Acids. 1. Binding to Nucleic Acid Components and to Single-Stranded Polynucleotides and Photocleavage of Single-Stranded Oligonucleotides†

A. Slama-Schwok,‡,§ J. Jazwinski,‡ A. Bêrê,§ T. Montenay-Garestier,§ M. Rougée,§ C. Hélène,*,§ and J.-M. Lehn*,‡

Chimie des Interactions Moléculaires, Collège de France, 11 Place Marcelin-Berthelot, 75005 Paris, France, and Laboratoire de Biophysique, Muséum National d'Histoire Naturelle, 43 Rue Cuvier, 75231 Paris Cedex 05, France

Received September 28, 1988

ABSTRACT: The binding of dimethyldiazaperopyrenium dication (**1**) with nucleosides, nucleotides, and single-stranded polynucleotides has been studied by photophysical methods. It has been shown that **1** may be a potential selective fluorescent probe for A- and/or T-rich polynucleotides. **1** efficiently cleaves oligonucleotides at guanine sites, under illumination with visible light, and therefore may be used as a sequence-specific artificial photonuclease.

Cationic planar molecules such as the acridine dyes (Neidle & Waring, 1983; Steiner & Kubota, 1983; Berman & Young, 1981; Zimmerman, 1986; Dougherty & Pilbrow, 1984) and neutral aromatic polycyclic molecules such as pyrene (Lianos & Georghiou, 1979; Zinger & Geacintov, 1988) are known to interact and form complexes with DNA and its constituents. In the present work, we have studied the interactions of the dimethyldiazaperopyrenium[1] dication (**1**) with nucleosides, nucleotides, and single-stranded polynucleotides. It has been

† The Ministère des Affaires Étrangères is acknowledged for the attribution of a Post-Doctoral Fellowship to A.S.-S.

‡ Collège de France.

§ Muséum National d'Histoire Naturelle.

[1] The diazaperopyrene is first described in the literature in German Patent 276.357 (June 1913). Aromatische Kohlenwasserstoffe (MC 18), Dr. E. Clar, Berlin Springer-Verlag, 1941.

0006-2960/89/0428-3227$01.50/0